



This open access document is posted as a preprint in the Beilstein Archives at <https://doi.org/10.3762/bxiv.2023.11.v1> and is considered to be an early communication for feedback before peer review. Before citing this document, please check if a final, peer-reviewed version has been published.

This document is not formatted, has not undergone copyediting or typesetting, and may contain errors, unsubstantiated scientific claims or preliminary data.

Preprint Title Non-peptide compounds from *Kromopolites svenhedini* (Verhoeff) and their anti-tumor and iNOS inhibitory activities

Authors Yuan-Nan Yuan, Jin-Qiang Li, Hong-Bin Fang, Shao-Jun Xing, Yong-Ming Yan and Yong-Xian Cheng

Publication Date 06 Apr. 2023

Article Type Full Research Paper

Supporting Information File 1 Supporting Information.pdf; 6.4 MB

ORCID® IDs Yong-Ming Yan - <https://orcid.org/0000-0003-4542-0431>

License and Terms: This document is copyright 2023 the Author(s); licensee Beilstein-Institut.

This is an open access work under the terms of the Creative Commons Attribution License (<https://creativecommons.org/licenses/by/4.0>). Please note that the reuse, redistribution and reproduction in particular requires that the author(s) and source are credited and that individual graphics may be subject to special legal provisions.

The license is subject to the Beilstein Archives terms and conditions: <https://www.beilstein-archives.org/xiv/terms>.

The definitive version of this work can be found at <https://doi.org/10.3762/bxiv.2023.11.v1>

Non-peptide compounds from *Kromopolites svenhedini* (Verhoeff) and their anti-tumor and iNOS inhibitory activities

Yuan-Nan Yuan^{1,2}, Jin-Qiang Li^{2,3}, Hong-Bin Fang², Shao-Jun Xing³, Yong-Ming Yan^{2*}, and Yong-Xian Cheng^{1,2**}

Address: ¹ School of Pharmacy, Guangdong Pharmaceutical University, Guangzhou 510006, PR China. ² Institute for Inheritance-Based Innovation of Chinese Medicine, School of Pharmaceutical Sciences, Health Science Center, Shenzhen University, Shenzhen 518060, PR China. ³ Department of Pathogen Biology, Health Science Center, Shenzhen University, Shenzhen 518060, PR China.

Email: Yong-Ming Yan - yanym@szu.edu.cn; Yong-Xian Cheng - yxcheng@szu.edu.cn

* Corresponding author

Abstract

Six new compounds, including one tetralone (**1**), two xanthenes (**2** and **3**), one flavan derivative (**4**), and two nor-diterpenoids (**7** and **8**), with two known flavan derivatives (**5** and **6**) and one known olefine acid (**9**) were isolated from the whole bodies of *Kromopolites svenhedini* (Verhoeff). All the structures of new compounds were determined by 1D and 2D nuclear magnetic resonance (NMR) and other spectroscopic methods, as well as computational methods. Part of the compounds were evaluated for their biological properties against the mouse pancreatic cancer cell line and inhibitory effects on iNOS and COX-2.

Keywords

Kromopolites svenhedini (Verhoeff); arthropod; non-peptide small molecules; anti-tumor; iNOS

Introduction

Millipede *Kromopolites svenhedini* (Verhoeff) ubiquitous in nature and common in our living environment, is a type of arthropod and plays the role of the decomposer in forest ecosystems [1]. In ancient China, there were abundant records about the using of animals and insects, homology of medicine and food. Millipede, a traditional Chinese medicine, has anti-inflammatory, analgesia, soothing the stomach, and relieve tiredness effects [2]. Most of the recent researches about millipede are in biological sciences and environmental science, such as their community changes [3–5]. According to very few studies on the chemical composition and biological activity about millipede, we can find that it contains antimicrobial peptides [6], defensive alkaloids [7],

and defensive long chain alcohol acetates [8]. In our studies of arthropods and insects over the years, we have found that non-peptide small molecules play an important part in chemical structures and biological activities [9–14].

Therefore, when it came to the chemical constituents in millipede *Kromopolites svenhedini* (Verhoeff), we focused on the non-peptide small molecules, and isolated six new compounds (kromopoiols A–D and kromoponoids A and B) and three known compounds from its extract. These structures were determined by 1D and 2D NMR spectra and the experimental and calculated electronic circular dichroism (ECD) spectra. Biological activity experiments were performed for isolated compounds, and the result shows that compound **4** had anti-tumor activity against Panc02-h7-GP-GFP (a mouse pancreatic cancer cell line) cells in a dose-dependent manner, and **5** shows anti-tumor activity at 40 μ M. Compounds **3–5** decreased the expression of iNOS and showed some dose-dependence.

Results and Discussion

Structural Identification

Compound **1**, yellow gum, has the molecular formula $C_{14}H_{18}O_4$ (six degrees of unsaturation) deduced from its HRESIMS $[M + H]^+$ ion at m/z 251.1274 (calcd for $C_{14}H_{19}O_4$, 257.1278), ^{13}C NMR, and DEPT data. The 1H NMR data (Table 1 and Figure S1 in Supporting Information File 1) displays one aromatic proton [δ_H 7.02 (1H, s, H-7)], two methoxy signals [δ_H 3.96 (3H, s, H₃-12) and 3.73 (3H, s, H₃-11)], and two methyl signals [δ_H 2.51 (3H, s, H₃-10) and 1.09 (3H, d, $J = 6.8$ Hz, H₃-9)]. The ^{13}C NMR and DEPT spectra of **1** (Table 1 and Figure S2 in Supporting Information File 1) contain 14 resonances attributable to two methyls, two methoxy carbons, one methylene, three

methines (one sp^2 and one oxygenated), one ketone, and five sp^2 carbons (two oxygenated). Some of these signals resemble those of 8-O-methylteratosphaerone B [15], indicating that they are analogues, but differing in benzene ring with an additional methyl group in **1**. The HMBC correlations (Figure 2 and Figure S5 in Supporting Information File 1) of H₃-10/C-4 (δ_c 72.9, weak), C-4a (δ_c 136.1), C-5 (δ_c 124.5), C-6 (δ_c 148.5) disclosed that C-10 is connected to C-5 in **1**. The coupling constant was used to deduce the relative configuration of the cyclohexanone segment in **1**. The small coupling constant ($J_{3,4} = 3.0$ Hz) revealed that H-3 and H-4 are on the same side of the ring, which was supported according to the literature [16]. The absolute configuration of **1** was identified as *3R,4R* according to accordance of the experimental and calculated ECD spectra (Figure 3 and Figure S7 in Supporting Information File 1). Therefore, the structure of **1** was defined and named as kromopoiol A.

Compound **2**, brown solid, has the molecular formula C₁₇H₁₆O₆ (ten degrees of unsaturation) deduced from its HRESIMS [M + H]⁺ ion at m/z 317.1008 (calcd for C₁₇H₁₇O₆, 317.1020), ¹³C NMR, and DEPT data. The ¹H NMR data (Table 2 and Figure S8 in Supporting Information File 1) displays one aromatic signal [δ_H 7.47 (2H, s, H-1, H-8)], one methoxy signal [δ_H 3.95 (6H, s, H₃-11, H₃-14)], and one methyl signal [δ_H 2.48 (6H, s, H₃-12, H₃-13)]. The ¹³C NMR and DEPT spectra of **2** (Table 2 and Figure S9 in Supporting Information File 1) contain 9 resonances attributable to one methyl, one methoxy carbon, one sp^2 methine, one ketone, and five sp^2 carbons (three oxygenated). The ¹H and ¹³C NMR data and the molecular formula indicated that it possesses two same pentasubstituted benzene rings, in other words, this compound has an axially symmetric structure. The methoxy group is positioned at C-3 according to the HMBC correlation (Figure 2 and Figure S12 in Supporting Information File 1) of H₃-11/C-3 (δ_c 154.1). The HMBC correlations of H-1/C-2 (δ_c 148.7), C-9a (δ_c 118.1),

C-9 (δ_c 178.5), and H₃-12/C-3, C-4 (δ_c 121.6), C-4a (δ_c 151.0), C-11 (δ_c 61.0, weak), disclosed that the hydroxy group and the methyl group are positioned at C-2 and C-4, respectively, by the literature [17–20]. On the basis of the above results, the other benzene ring has same structure. Comparing the ¹H and ¹³C chemical shifts with similar compounds [17–20], the NMR information indicates the presence of C-8a-C-9-C-9a and C-4a-O-C-10a bonds in the structure of **2**. Therefore, the structure of **2** was defined and named as kromopoiol B.

Compound **3**, brown solid, has the molecular formula C₁₅H₁₂O₄ (ten degrees of unsaturation) deduced from its HRESIMS [M + H]⁺ ion at *m/z* 257.0802 (calcd for C₁₅H₁₃O₄, 257.0808), ¹³C NMR, and DEPT data. The ¹H NMR data (Table 2 and Figure S14 in Supporting Information File 1) displays one typical AB spin system [δ_H 7.47 (1H, s, H-1), 7.39 (1H, d, *J* = 1.0 Hz, H-4)], corresponding to a 1,2,4,5-tetrasubstituted benzene substructure. Additional aromatic proton signals [δ_H 7.38 (1H, d, *J* = 3.1 Hz, H-8) and δ_H 7.16 (1H, dd, *J* = 3.4, 1.0 Hz, H-6)] suggested the presence of a 1,2,3,5-tetrasubstituted benzene substructure. The ¹³C NMR and DEPT spectra of **3** (Table 2 and Figure S15 in Supporting Information File 1) contain 15 resonances attributable to two methyls, four sp² methines, one ketone, and eight sp² carbons (four oxygenated). The two methoxy groups are positioned at C-3 and C-5 according to the HMBC correlations (Figure 2 and Figure S18 in Supporting Information File 1) of H₃-11/C-2 (δ_c 153.8), C-3 (δ_c 137.5), C-4 (δ_c 120.5) and H₃-12/C-5 (δ_c 130.2), C-6 (δ_c 126.1), C-10a (δ_c 150.1), C-8a (δ_c 61.0, weak). By the literature [17–20], the HMBC correlations of H-1/C-2, C-9a (δ_c 120.5), C-9 (δ_c 179.1) and H-8/C-7 (δ_c 154.4), C-9 (δ_c 179.1) disclosed that the hydroxy groups are positioned at C-2 and C-7, respectively. Comparing with similar **2**, **3** also has C-8a-C-9-C-9a and C-4a-O-C-10a bonds. Therefore, the structure of **3** was defined and named as kromopoiol C.

Compound **4**, brown solid, has the molecular formula $C_{21}H_{24}O_5$ (six degrees of unsaturation) deduced from its HRESIMS $[M + H]^+$ ion at m/z 357.1680 (calcd for $C_{21}H_{25}O_5$, 357.1697), ^{13}C NMR, and DEPT data. The 1H NMR data (Table 3 and Figure S20 in Supporting Information File 1) contains three typical aromatic signals [δ_H 6.86 (1H, m, H-5, overlap), 6.31 (1H, dd, $J = 8.2, 2.4$ Hz, H-6), and 6.26 (1H, d, $J = 2.4$ Hz, H-8)], suggesting the presence of a 1,2,4-trisubstituted benzene substructure. In addition, two aromatic signals at δ_H 6.86 (1H, m, H-2', overlap) and δ_H 6.84 (1H, s, H-6') were also observed in the 1H NMR spectrum, indicating the presence of a 1,2,4,5-tetrasubstituted benzene substructure. The ^{13}C NMR and DEPT spectra of **4** (Table 3 and Figure S21 in Supporting Information File 1) contain 21 resonances attributable to two methyls, one methoxy carbon, three methylenes, seven methines (five sp^2 and two oxygenated), one oxygenated proton, and seven sp^2 carbons (four oxygenated). Basing on above information, **4** was deduced to be similar with daphnegiralins C_1 [21], and they share the same 7-hydroxyflavan skeleton. The difference in **4** is an additional methoxy group, which is connected to C-5' supported by the HMBC correlation (Figure 2 and Figure S24 in Supporting Information File 1) of 5'-OCH₃ (δ_H 3.85)/C-5' (δ_C 136.1). There were two asymmetric carbon centers at C-2 and C-2'' in **4**. According to the literature [21], the absolute configuration at C-2 for **4** was assigned as *S*, from the Cotton effects in its ECD curve (Figure S26 in Supporting Information File 1) [283 nm ($\Delta\epsilon$ -0.71)]. The absolute configuration of **4** was determined as *2S,2''R* according to the accordance of the experimental and ECD spectra (Figure 3 and S26 in Supporting Information File 1). Therefore, the structure of **4** was defined and named as kromopoiol D.

Compound **7**, light yellow gum, has the molecular formula C₁₆H₂₈O₃ (three degrees of unsaturation) deduced from its HRESIMS [M + H]⁺ ion at *m/z* 251.1274 (calcd for C₁₆H₂₉O₃, 251.1278), ¹³C NMR, and DEPT data. The ¹H NMR spectrum (Table 4 and Figure S27 in Supporting Information File 1) displays two olefinic protons [δ_{H} 5.18 (1H, t, *J* = 7.0 Hz, H-10) and 5.12 (1H, t, *J* = 7.0 Hz, H-6)], two methoxy signals [δ_{H} 3.59 (2H, t, *J* = 7.1 Hz, H₂-13)], and three methyl signals [δ_{H} 1.63 (3H, s, H₃-16), 1.61 (3H, s, H₃-15), and 0.96 (3H, s, H₃-14)]. The ¹³C NMR and DEPT spectra of **7** (Table 4 and Figure S28 in Supporting Information File 1) contain 16 resonances attributable to three methyls, seven methylenes (one oxygenated), three methines (two sp²), one carbonyl carbon, and two sp² carbons. The ¹H–¹H COSY spectrum (Figure 2 and Figure S29 in Supporting Information File 1) of **7** showed the existence of correlations of H₂-2 (δ_{H} 2.29, 2.08)/H-3 (δ_{H} 1.91, 1.93)/H₂-4 (δ_{H} 1.38, 1.24)/H₂-5 (δ_{H} 2.03, 2H)/H-6 (δ_{H} 5.12), H-3 (δ_{H} 1.93)/H₂-15 (δ_{H} 0.96), H₂-8 (δ_{H} 2.03, 2H)/H₂-9 (δ_{H} 2.11, 2H)/H-10 (δ_{H} 5.18), and H₂-12 (δ_{H} 2.20, 2H)/H₂-13 (δ_{H} 3.59, 2H), which revealed three partial structures **a** (C-2 to C-6), **b** (C-8 to C-10), and **c** (C-12 to C-13). The partial structures **a** and **b** were connected to C-7 by the correlations of H₃-16 (δ_{H} 1.61)/C-6 (δ_{C} 125.6), C-7 (δ_{C} 136.0), C-8 (δ_{C} 40.7) and H-8/C-6, C-7 in HMBC spectrum (Figure 2 and Figure S31 in Supporting Information File 1). The partial structures **b** and **c** were connected to C-11, as confirmed by the HMBC correlations of H₃-17 (δ_{H} 1.63)/C-10 (δ_{C} 127.4), C-11 (δ_{C} 132.9), C-12 (δ_{C} 43.8) and H-12/C-10, C-11. The presence of a conjugated carboxylic acid was verified by the HMBC correlation of H₂-2 to C-1 (δ_{C} 177.1). As for the geometry of **7**, the ROESY correlation (Figure 2 and Figure S32 in Supporting Information File 1) of H-10/H₂-12 revealed that the $\Delta^{10,11}$ was *E* configuration. However, the signals of H₂-5 and H₂-8 overlap so badly that we cannot determine the geometry of the $\Delta^{6,7}$ by the same way. After we compared the ¹H and ¹³C chemical shifts with similar compounds [22–26], the geometry of the $\Delta^{6,7}$ was determined as *E*.

The configuration at C-3 was unable to determine on account of its long carbon chain. Therefore, the structure of **7** was defined and named as kromoponoid A.

Compound **8**, light yellow gum, has the molecular formula $C_{17}H_{30}O_3$ (three degrees of unsaturation) deduced from its HRESIMS $[M + H]^+$ ion at m/z 283.2268 (calcd for $C_{17}H_{31}O_3$, 283.2268), ^{13}C NMR, and DEPT data. The 1H NMR data (Table 4 and Figure S34 in Supporting Information File 1) displays two olefinic protons [δ_H 5.16 (2H, m, H-6, H-10)], two methoxy signals [δ_H 3.97 (2H, t, $J = 6.6$ Hz, H₂-14)], and three methyl signals [δ_H 1.61 (6H, s, H₃-16, H₃-17), and 0.94 (3H, d, $J = 6.2$ Hz, H₃-15)]. The ^{13}C NMR and DEPT spectra of **8** (Table 4 and Figure S35 in Supporting Information File 1) contain 17 resonances attributable to three methyls, eight methylenes (one oxygenated), three methines (two sp^2), one carbonyl carbon, and two sp^2 carbons. Analysis of the NMR data (Table 5), compared with that of **7**, indicated that both compounds possess the same general skeleton structure and the only difference was an additional methine group in **8**. The 1H - 1H COSY correlations (Figure 2 and Figure S36 in Supporting Information File 1) of H₂-12 (δ_H 1.98, 2H)/ H₂-13 (δ_H 2.08, 2H)/ H₂-14 (δ_H 3.97, 2H) and the HMBC correlations (Figure 2 and Figure S38 in Supporting Information File 1) of H-12/C-10 (δ_C 126.0), C-11 (δ_C 135.2) and H-13/C-11 showed the structure of C-12 to C-14, which is different from **7**. Because the signals between H₂-5 and H₂-8, H₂-9 and H₂-12 are overlap, the geometry of the double bonds was determined as *6E,10E* by comparison of the 1H and ^{13}C chemical shifts with similar compounds [22–26]. The configuration at C-3 was unable to determine on account of its long carbon chain. Therefore, the structure of **8** was defined and named as kromoponoid B.

Of note, the structures of **2–4** are common in plants but rare in animals. Whether these compounds are originated from plants or animals so far remains unknown. One fact is that a dozen of coumarins and their glucosides have been characterized from *Periplaneta americana* [27–29], reminding that compounds **2–4** might be synthesized by the title insect and there exists a biosynthetic pathway thereof.

The three known compounds were respectively identified as daphnegiralin C₁ (**5**) [21], daphnegiranol C₁ (**6**) [30], and (*E*)-oct-2-enoic acid (**9**) [31], by comparison of their spectroscopic data with those in the literature.

Biological Evaluation

To investigate the bioactive potential of isolated compounds, the cytotoxic and anti-inflammatory properties were evaluated. Especially, a mouse pancreatic cancer cell line (Panc02-h7-GP-GFP) was used to determine the cytotoxicity, and also measured response of enhancing effect on the function of CD8⁺ T cells with respect to compounds. In addition, LPS-induced pro-inflammatory expression of iNOS and COX-2 in RAW264.7 cells were evaluated.

Anti-tumor activity of compounds **2–5** was evaluated by the cell proliferation assay on Panc02-h7-GP-GFP cells. It was found that compound **4** exhibited cytotoxic activity towards Panc02-h7-GP-GFP cells at concentrations of 10, 20, and 40 μ M in a dose-dependent manner and **5** exhibited weak cytotoxic activity at 40 μ M (Figure 4). In other hand, the enhancement of CD8⁺ T cells were studied corresponding concentration of compounds **2–5**. Unfortunately, we did not find any enhancement of CD8⁺ T cells (Figure S42 in Supporting Information File 1).

Meanwhile, compounds **1–5**, **7**, and **8** were evaluated for their anti-inflammatory activity against pro-inflammatory expression of iNOS and COX-2. The result shows that compounds **3–5** exhibited inhibitory effects towards LPS-induced iNOS in RAW264.7 cells with dose-dependent manner (Figure 5 A–C). Whereas, all the tested compounds were inactive against LPS-induced COX-2 in RAW264.7 cells. To examine the toxicity of compounds **1–5**, **7**, and **8**, the CCK-8 assay used to detect the viability of RAW264.7 cells. The result indicates that the compounds do not show significant toxicity toward RAW264.7 cells at the indicated concentrations (Figure 5 D and E). In contrast, compounds **1**, **2**, **7**, and **8** could promote proliferation of RAW264.7 cells at 20 μ M.

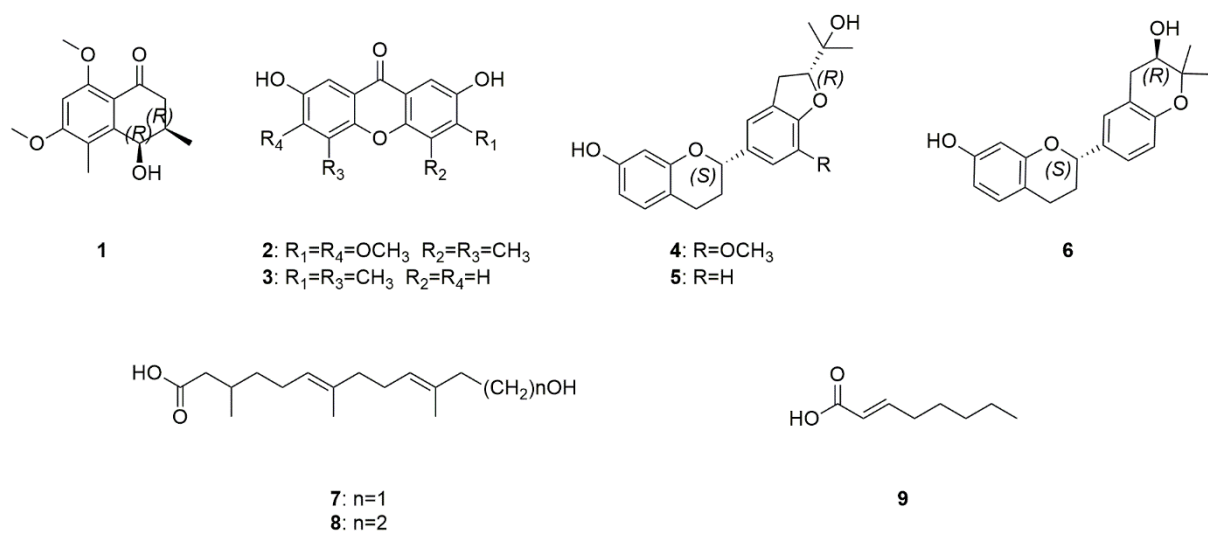


Figure 1: Structures of compounds 1–9.

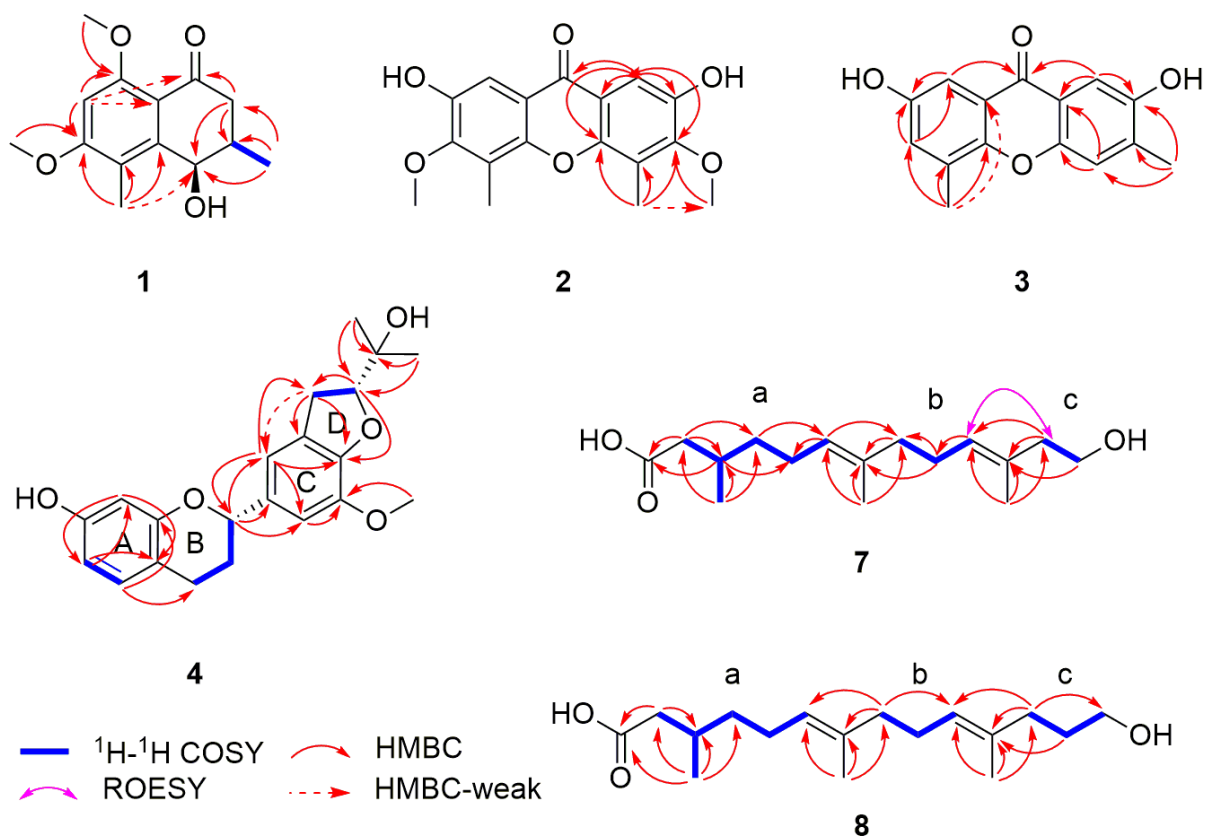


Figure 2: Key ^1H - ^1H COSY, HMBC, and ROESY correlations of **1–4**, **7**, and **8**.

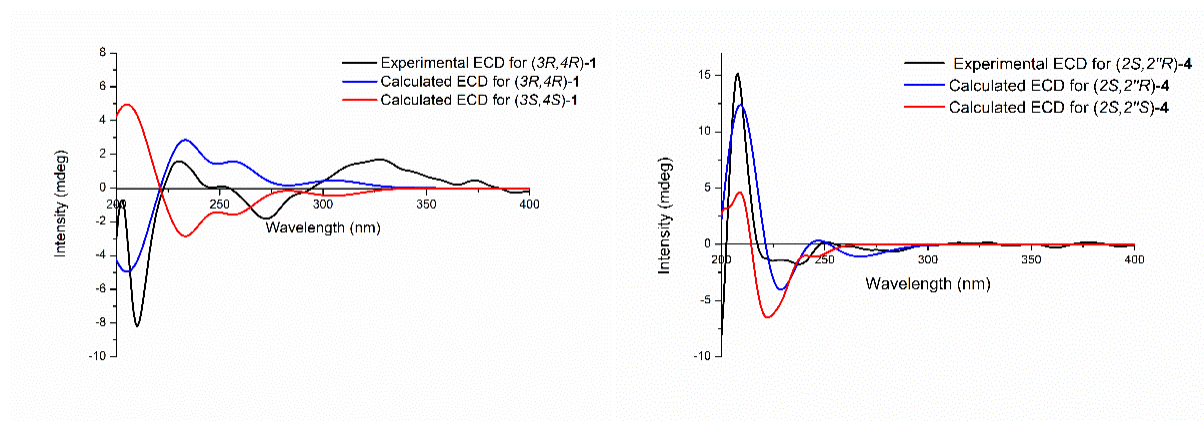


Figure 3: Calculated and experimental ECD spectra of **1** and **4**.

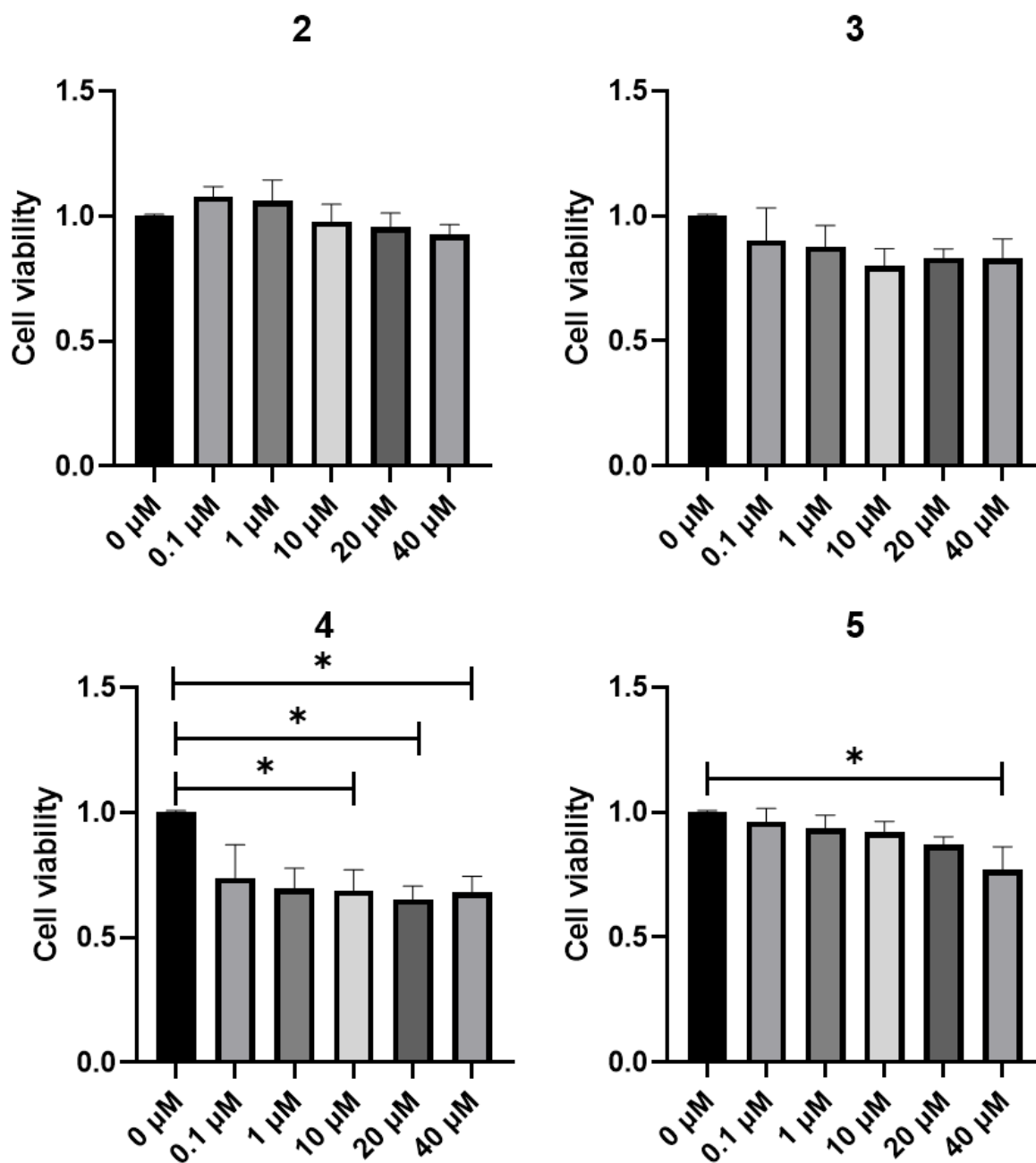


Figure 4: Compounds **4** and **5** exhibited cytotoxic activity towards Panc02-h7-GP-GFP cells. Cells were incubated with the corresponding concentration of compounds or DMSO for 18 h. CCK-8 assay was used to determine cell viability. * $p < 0.05$ compared with DMSO alone.

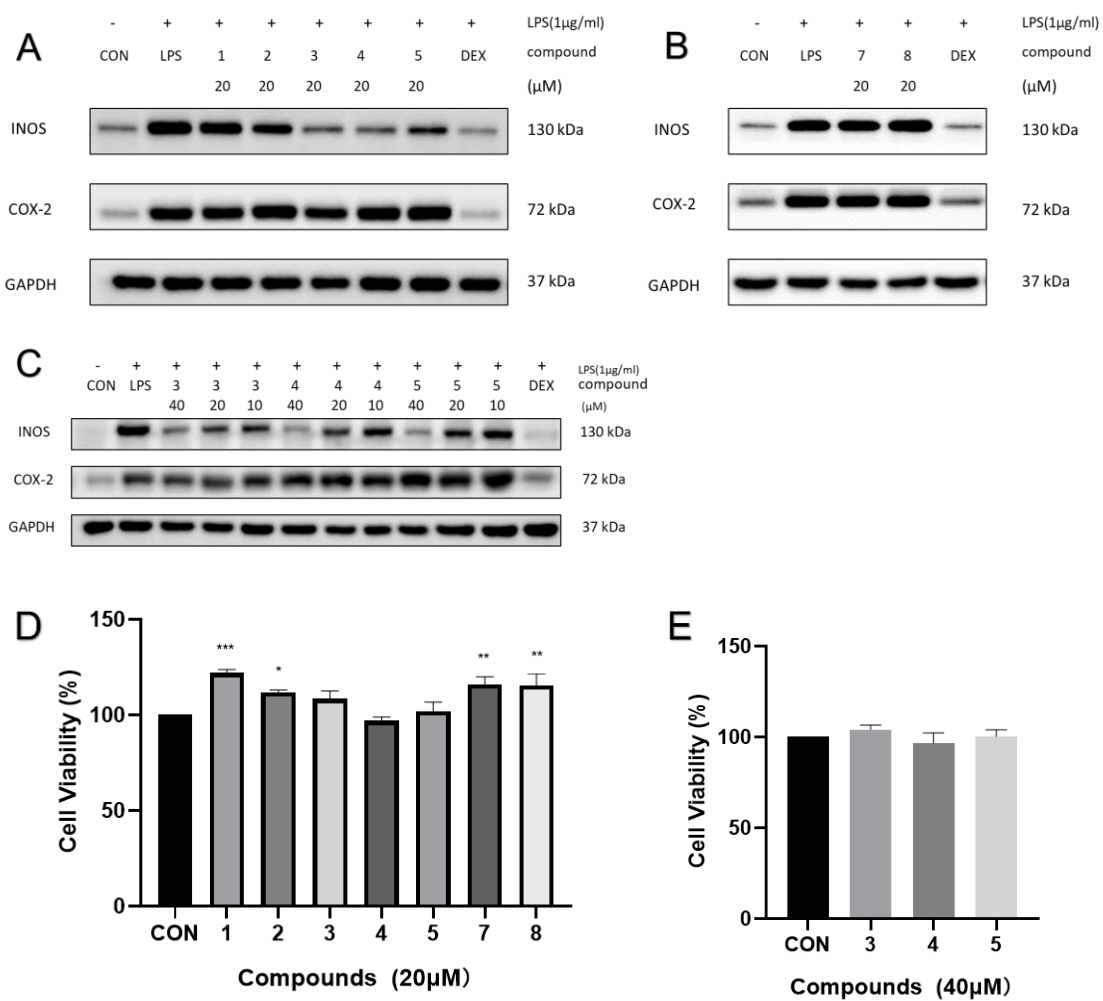


Figure 5: Compounds 3–5 inhibited the expression of the LPS-induced pro-inflammatory expression of iNOS in RAW264.7 cells. Cells were treated with the corresponding concentration of compounds or DMSO for 2 h before exposed to 1 $\mu\text{g}/\text{mL}$ LPS for 12 h. **A–C**, western blotting was used to determine the protein levels of iNOS and COX-2, with GAPDH as a control and dexamethasone (DEX) as a positive drug. **D** and **E**, the proliferation of RAW264.7 cells in response to compounds at 20 and 40 μM was assessed by CCK-8 assay. Data represent mean \pm SEM values of three experiments. * $p < 0.05$, ** $p < 0.01$, and *** $p < 0.001$ compared with CON group (DMSO alone).

Table 1: ^1H (600 MHz) and ^{13}C NMR (150 MHz) data of **1** (δ in ppm, J in Hz, methanol- d_4).

No.	δ_{H} (mult, J , amount)	δ_{C} mult	No.	δ_{H} (mult, J , amount)	δ_{C} mult
C-1		201.3 C	C-7	7.02 (s, 1H)	110.8 CH
C-2	2.64 (dd, $J = 17.2, 10.3, 1\text{H}$) 2.48 (dd, $J = 17.2, 4.7, 1\text{H}$)	43.7 CH ₂	C-8		158.0 C
C-3	2.36 (m, 1H)	35.8 CH	C-8a		145.6 C
C-4	4.69 (d, $J = 3.0, 1\text{H}$)	72.9 CH	C-9	1.09 (d, $J = 6.8, 3\text{H}$)	16.3 CH ₃
C-4a		136.1 C	C-10	2.51 (s, 3H)	14.1 CH ₃
C-5		124.5 C	C-11	3.73 (s, 3H)	60.7 CH ₃
C-6		148.5 C	C-12	3.96 (s, 3H)	56.3 CH ₃

Table 2: ^1H (600 MHz) and ^{13}C NMR (150 MHz) data of **2** and **3** (δ in ppm, J in Hz, methanol- d_4).

No.	2		3	
	δ_{H} (mult, J , amount)	δ_{C} mult	δ_{H} (mult, J , amount)	δ_{C} mult
C-1	7.47 (s, 1H, overlap)	108.3 CH	7.47 (s, 1H)	108.2 CH
C-2		148.7 C		153.8 C
C-3		154.1 C		137.5 C
C-4		121.6 C	7.39 (d, $J = 1.0$, 1H)	120.5 CH
C-4a		151.0 C		151.6 C
C-5		121.6 C		130.2 C
C-6		154.1 C	7.16 (dd, $J = 3.1, 1.0$, 1H)	126.1 CH
C-7		148.7 C		154.4 C
C-8	7.47 (s, 1H, overlap)	108.3 CH	7.38 (d, $J = 3.1$, 1H)	107.2 CH
C-8a		118.1 C		122.5 C
C-9		178.5 C		179.1 C
C-9a		118.1 C		120.5 CH
C-10a		151.0 C		150.1 C
C-11	3.95 (s, 3H, overlap)	61.0 CH ₃	2.37 (s, 3H)	17.1 CH ₃
C-12	2.48 (s, 3H, overlap)	9.2 CH ₃	2.52 (s, 3H)	15.8 CH ₃
C-12	2.48 (s, 3H, overlap)	9.2 CH ₃		
C-14	3.95 (s, 3H, overlap)	61.0 CH ₃		

Table 3: ^1H (500 MHz) and ^{13}C NMR (150 MHz) data of **4** (δ in ppm, J in Hz, methanol- d_4).

No.	δ_{H} (mult, J , amount)	δ_{C} mult	No.	δ_{H} (mult, J , amount)	δ_{C} mult
C-2	4.92 (m, 1H)	79.2 CH	C-3'		129.8 C
C-3	2.12 (m, 1H)	31.6 CH ₂	C-4'		149.2 C
	2.00 (m, 1H)				
C-4	2.86 (ddd, $J = 16.5, 11.3,$ 5.7, 1H)	25.5 CH ₃	C-5'		145.2 CH
	2.67 (m, 1H)				
C-5	6.86 (m, 1H, overlap)	131.0 CH	C-6'	6.84 (s, 1H)	111.4 CH
C-6	6.31 (dd, $J = 8.2, 2.4,$ 1H)	109.1 CH	C-1''	3.19 (m, 2H)	32.0 CH ₂
C-7		157.6 C	C-2''	4.63 (t, $J = 9.0,$ 1H)	91.1 CH
C-8	6.26 (d, $J = 2.4,$ 1H)	104.1 CH	C-3''		72.5 C
C-9		157.1 C	C-4''	1.24 (s, 3H)	25.5 CH ₃
C-10		114.3 C	C-5''	1.26 (s, 3H)	25.0 CH ₃
C-1'		136.5 C	5'-	3.85 (s, 3H)	56.8 CH ₃
			OCH ₃		
C-2'	6.86 (m, 1H, overlap)	116.2 CH			

Table 4: ^1H (500 MHz) and ^{13}C NMR (150 MHz) data of **7** and **8** (δ in ppm, J in Hz, methanol- d_4).

No.	7		8	
	δ_{H} (mult, J , amount)	δ_{C} mult	δ_{H} (mult, J , amount)	δ_{C} mult
C-1		177.1 C		182.5 C
C-2	2.29 (dd, $J = 14.8, 6.0, 1\text{H}$) 2.08 (m, 1H)	42.6 CH ₂	2.19 (m, 1H) 1.94 (m, 1H, overlap)	47.3 CH ₂
C-3	1.93 (m, 1H)	31.1 CH	1.94 (m, 1H, overlap)	32.2 CH
C-4	1.38 (m, 1H) 1.24 (m, 1H)	37.8 CH ₂	1.38 (m, 1H) 1.19 (m, 1H)	38.5 CH ₂
C-5	2.03 (m, 2H, overlap)	26.3 CH ₂	2.02 (m, 1H) 1.98 (m, 1H, overlap)	26.6 CH ₂
C-6	5.12 (t, $J = 7.0, 1\text{H}$)	125.6 C	5.16 (m, 1H, overlap)	126.0 CH
C-7		136.0 C		135.6 C
C-8	2.03 (m, 2H, overlap)	40.7 CH ₂	1.98 (m, 2H, overlap)	40.9 CH ₂
C-9	2.11 (m, 2H, overlap)	27.6 CH ₂	2.08 (m, 2H, overlap)	27.9 CH ₂
C-10	5.18 (t, $J = 7.0, 1\text{H}$)	127.4 C	5.16 (m, 1H, overlap)	126.0 CH
C-11		132.9 C		135.2 C
C-12	2.20 (m, 2H, overlap)	43.8 CH ₂	2.08 (m, 2H, overlap)	36.8 CH ₂
C-13	3.59 (t, $J = 7.1, 2\text{H}$)	61.9 CH ₂	1.75 (m, 2H)	29.0 CH ₂
C-14			3.97 (t, $J = 6.6, 2\text{H}$)	68.9 CH ₂
C-15	0.96 (s, 3H)	20.0 CH ₃	0.94 (d, $J = 6.2, 3\text{H}$)	20.3 CH ₃
C-16	1.61 (s, 3H)	16.0 CH ₃	1.61 (s, 3H, overlap)	16.1 CH ₃
C-17	1.63 (s, 3H)	16.3 CH ₃	1.61 (s, 3H, overlap)	16.0 CH ₃

Conclusion

Six new and three known non-peptide small molecules were isolated from the millipede *Kromopolites svenhedini* (Verhoeff), and their structures were characterized by spectroscopic and calculated methods. Biological evaluation of compounds **4** and **5** indicated that they have the anti-tumor activity against Panc02-h7-GP-GFP cells and compounds **3–5** had inhibitory activities against LPS-induced iNOS in RAW264.7 cells. These findings add new contributions to the chemistry and biological activity of arthropod-derived non-peptide small molecules.

Experimental

General

1D and 2D NMR spectra were performed on Bruker AV-500 and AV-600 spectrometer (Bruker) in which tetramethylsilane (TMS) was used as an internal standard. HRESIMS was obtained by a Shimadzu LC-20 CE AB SCIEX QTOF X500R MS spectrometer (Shimadzu Corporation, Tokyo, Japan). Optical rotations (ORD) were collected on a Horiba SEPA-300 polarimeter. Ultraviolet (UV) and Circular dichroism (CD) spectra were carried out on a Jasco J-815 CD spectrometer (JASCO). For column chromatography (CC), macroporous adsorbent resin Amberlite TM XAD 16N (particle size 20–60 mesh, Rohm and Haas Company), MCI gel CHP 20P (particle size 75–150 μm , Mitsubishi Chemical Industries, Japan), RP-18 (particle size 40–60 μm ; Daiso Co.), C-18 silica gel (particle size 40–60 μm ; Daiso Co., Japan), Sephadex LH-20 (Amersham Biosciences), and YMC gel ODS-A-HG (particle size 40–60 μm ; YMC Co. Japan). A Saipuruisi chromatograph with Semi-preparative high-pressure infusion pump (SP-5030) and Semi-preparative UV-vis dual wavelength detector (UV200) was

used for RP-HPLC. A YMC-Pack ODS-A column (250 mm × 20 mm, i.d., S-5 μm) for preparative HPLC, and three columns (a YMC-Pack ODS-A column (250 mm × 10 mm, i.d., 5 μm), a Stabllity 100 C30 column (25 mm × 10 mm, i.d., 5 μm), and an Inetex-Biphenyl 100A column (250 mm × 10 mm, i.d., 5 μm)) for semipreparative HPLC was used.

Insect Material

The dry arthropod bodies of *Kromopolites svenhedini* (Verhoeff) were purchased from Qunkang Pharmaceutical Co. in Anhui Province, PR China, in July 2021. The voucher specimen of this material (CHYX-0674) was deposited at School of Pharmaceutical Sciences, Health Science Center, Shenzhen University, PR China.

Extraction and Isolation

The dried and powdered *Kromopolites svenhedini* (Verhoeff) (49 kg) was extracted with 50% EtOH (4 × 120 L, 24 h at a time) to give a crude extract. This extract was divided into six parts (Fr.A–Fr.F) using a macroporous adsorbent resin column eluted with gradient aqueous MeOH (0%–100%). Fr.E (180 g) was divided into four portions (Fr.E1–Fr.E9, Fr.EA) by using an MCI gel CHP 20P column (MeOH/H₂O, 60%–100%). Fr.E2 (2.0 g) was divided into six portions (Fr.E21–Fr.E26) by Sephadex LH-20 (MeOH/H₂O, 70%). Fr.E25 (248.6 mg) was subjected to preparative HPLC (MeOH/H₂O (0.04% TFA), 50%–100%, flow rate: 10 mL min⁻¹) to give six portions (Fr.E251–Fr.E256). Fr.E254 was decompressed and concentrated to obtain compound **9** (20.00 mg). And Fr.E255 (51.8 mg) was further purified using semi-preparative HPLC (C30, MeOH/H₂O, 25%, flow rate: 3mL min⁻¹) to yield compound **8** (16.23 mg, *t_R* = 25.04 min). Fr.E5 (9.0 g) was divided into eleven portions (Fr.E51–Fr.E59, Fr.E5A–B) by Sephadex LH-20 (MeOH/H₂O, 70%). Fr.E53 (4.26 g) was divided into eleven portions (Fr.E531–Fr.E539, Fr.E53A, Fr.E53B) by using an MCI gel

CHP 20P column (MeOH/H₂O, 10%–100%). Then, Fr.E537 (354.8 mg) was divided into three portions (Fr.E5371–Fr.E5373) by Sephadex LH-20 (MeOH). Fr.E5373 (216.6 mg) was further fractionated into eight parts by a silica gel column (PE–EtOAc, 2:1–1:1, to DCM/MeOH, 20:1–1:1), and Fr.E53732 (63.8 mg) was further purified by using semi-preparative HPLC (ODS-A, MeCN/H₂O (0.04% TFA), 55%, flow rate: 3 mL min⁻¹) to afford compound **7** (15.70 mg, t_R = 14.05 min). Fr.E54 (415.3 mg) was divided into twelve portions (Fr.E541–Fr.E549, Fr.E54A–Fr.E54C) by using an MCI gel CHP 20P column (MeOH/H₂O, 30%–100%), followed by semi-preparative HPLC (ODS-A, MeCN/H₂O (0.04% TFA), 28%, flow rate: 3 mL min⁻¹) to produce compound **1** (1.32 mg, t_R = 27.89 min). Fr.E8 (13.1 g) was divided into five portions (Fr.E81–Fr.E85) by Sephadex LH-20 (MeOH). Fr.E84 (207.3 mg) was divided into thirteen portions (Fr.E841–Fr.E849, Fr.E84A–Fr.E84D) by using an ODS-A-HG column (MeOH/H₂O, 30%–100%). Fr.E846 (21.4 mg) was purified by using semi-preparative HPLC (C30, MeCN/H₂O (0.04% TFA), 42%, flow rate: 3 mL min⁻¹) to afford compound **4** (0.97 mg, t_R = 51.45 min). Fr.E847 (21.4 mg) was purified by using semi-preparative HPLC (ODS-A, MeCN/H₂O (0.04% TFA), 40%, flow rate: 3 mL min⁻¹) to afford compound **5** (1.21 mg, t_R = 56.80 min) and compound **6** (1.16 mg, t_R = 61.32 min). Fr.E85 (686.7mg) was divided into ten portions (Fr.E851–Fr.E859, Fr.E85A) by using a RP-18 column (MeOH/H₂O, 30%–100%). Fr.E856 (31.3 mg) was purified by using semi-preparative HPLC (Inetex-Biphenyl, MeCN/H₂O (0.04% TFA), 38%, flow rate: 3 mL min⁻¹) to afford compounds **3** (0.99 mg, t_R = 25.33 min) and **2** (0.76 mg, t_R = 30.38 min).

Compound Characterization

Kromopiol A (1): yellow gum; [α]²⁵_D +9.38 (c 0.32, MeOH); UV (MeOH) λ_{max} (log ε) 208 (2.92), 229 (2.88), 275 (2.78) nm; ECD (MeOH) λ (Δ ε) 210 (-1.88), 231 (+0.34),

251 (+0.02), 273(-0.41), 327(+0.39) nm; HRESIMS [M + H]⁺ ion at *m/z* 251.1274 (calcd for C₁₄H₁₉O₄, 257.1278); ¹H and ¹³C NMR data, see Table 1.

Kromopoiol B (2): brown solid; UV (MeOH) λ_{max} (log ε) 202 (3.56), 242 (3.58), 280 (3.13), 324 (3.15), 367 (2.89) nm; HRESIMS [M + H]⁺ ion at *m/z* 317.1008 (calcd for C₁₇H₁₇O₆, 317.1020); ¹H and ¹³C NMR data, see Table 2.

Kromopoiol C (3): brown solid; UV (MeOH) λ_{max} (log ε) 201 (3.18), 241 (3.44), 260 (3.22), 324 (2.73), 378 (2.69) nm; HRESIMS [M + H]⁺ ion at *m/z* 257.0802 (calcd for C₁₅H₁₃O₄, 257.0808); ¹H and ¹³C NMR data, see Table 2.

Kromopoiol D (4): brown solid; [α]²⁵_D +30.77 (c 0.26, MeOH); UV (MeOH) λ_{max} (log ε) 207 (3.92), 280 (3.14) nm; ECD (MeOH) λ (Δε) 208(+15.19), 237(-1.90), 250(+0.23), 283(-0.71) nm; HRESIMS [M + H]⁺ ion at *m/z* 357.1680 (calcd for C₂₁H₂₅O₅, 357.1697); ¹H and ¹³C NMR data, see Table 3.

Kromoponoid A (7): light yellow gum; [α]²⁵_D +7.50 (c 0.40, MeOH); UV (MeOH) λ_{max} (log ε) 202 (3.68) nm; HRESIMS [M + H]⁺ ion at *m/z* 251.1274 (calcd for C₁₆H₂₉O₃, 251.1278); ¹H and ¹³C NMR data, see Table 4.

Kromoponoid B (8): light yellow gum; [α]²⁵_D +2.50 (c 0.40, MeOH); UV (MeOH) λ_{max} (log ε) 202 (3.81) nm; HRESIMS [M + H]⁺ ion at *m/z* 283.2268 (calcd for C₁₇H₃₁O₃, 283.2268); ¹H and ¹³C NMR data, see Table 4.

Computational Methods

The CONFLEX 7 searches in the light of Molecular Merck force field (MMFF94) and DFT/TDDFT, calculated with Spartan'14 software package and Gaussian 09 program package, were performed for model compounds of (3*R*,4*R*)-1, (3*S*,4*S*)-1, (2*S*,2"*R*)-4, and (2*S*,2"*S*)-4, respectively. The ECD calculations of the predominant conformers (80%) were subjected by DFT calculation at B3LYP/6-311G (d,p) level. The program SpecDis 1.62 was using to generated the CD spectra [32].

Biological Evaluation

Anti-tumor Assay

Panc02-h7-GP-GFP cells (obtained by transformation of mouse pancreatic cancer cell line Panc02-h7) were incubated at 37°C under 5% CO₂ atmosphere in high-glucose DMEM (GIBCO, USA) containing 10% fetal bovine serum (FBS, GIBCO, USA), 100 U/ml penicillin, 10 μg/ml streptomycin, and 10 μg/ml puromycin. Cells were seeded at 5000 cells/well in 96-well plates with same incubation conditions as before. After overnight culture, cells were pretreated with the corresponding concentration of compounds or DMSO for 18 h. Then Cell Count Kit-8 (CCK-8, MCE, USA) was added into each well at 10 μM for 2 h. Plates were recorded at 450 nm using a microplate reader (TECAN, Switzerland).

Anti-tumor Activity Assay of CD8⁺ T Cells in Vitro

This assay and included experimental procedures were approved by the Institutional Animal Care and Use Committee of Shenzhen University Health Science Center and Animal Experimentation Ethics Committee of Shenzhen University Health Science Center (AEWC-202300026). All animal housing and using were in accordance with the research ethics guidelines of the Institutional Animal Care and Use Committee of

Shenzhen University Health Science Center and Animal Experimentation Ethics Committee of Shenzhen University Health Science Center.

Panc02-h7-GP-GFP cells were digested with trypsin (0.25%, Sigma), resuspended by PBS (GIBCO, USA) after centrifuged. The cell suspension was injected into the pancreas of mice (1×10^6 cells per mouse). After 14 days, the tumors were taken out and digested by digestion solution, then ground and centrifuged to make a cell suspension. Lymphocytes obtained from the cell suspension by Percoll isolation method and were enriched (using negative selection) to obtain Naive CD8⁺ T cells. Enrichment effect and phenotype of CD8⁺ cells detected by flow cytometry (BD, USA). CD8⁺ T cells and Panc02-h7-GP-GFP cells were co-cultured with the corresponding concentration of compounds or DMSO for 18 h. The fluorescence intensity was detected by a microplate reader (emission light 476nm, excitation light 514nm).

Anti-inflammatory assay

RAW264.7 (a mouse macrophage cell line) cells were incubated in high-glucose DMEM (GIBCO, USA) containing 10% fetal bovine serum (FBS, GIBCO, USA), 100U/ml penicillin and 100 μ g/ml streptomycin. Cells were incubated with 5% CO₂ in air at 37 °C and then plated in 96-well plates at a concentration of 2×10^4 cells/well with same incubation conditions as before. After overnight incubation, the cells were incubated with the corresponding concentration of compound or DMSO for 24 h. CCK-8 (Beyotime, China) solution was added and incubated for 1 h. The absorbance of the solution in the 96-well plate was detected by a microplate reader (450nm, BioTek, USA) and the survival rate of the cells was calculated.

Western blot was used to detect protein levels in cells. The RAW264.7 cells were pre-treated with the corresponding concentration of compound or DMSO for 2 h and

stimulated with lipopolysaccharide (LPS, 1 μ g/mL) for 12 h. After it, radioimmunoprecipitation assay (RIPA) buffer (Beyotime, PR China) containing protease inhibitor (Roche, Germany) was using to extract total protein from cells. The content of protein samples was detected by BCA assay (Thermo, USA).

Equivalent protein extracts were isolated by 10% SDS-PAGE and transferred to PVDF membrane. The membranes were blocked with 5% BSA, then incubated with indicated antibodies overnight at 4 °C. Finally, the membranes were incubated with horseradish peroxidase (HRP)-conjugated secondary antibody at room temperature. The ECL kit (Pierce, USA) and analysis system (Bio-Rad, CA, USA) were using to visualize and detect the bands. Results of immunoblot densitometric analysis was performed by ImageJ software (NIH, USA).

Supporting Information

Supporting Information File 1: NMR, HRESIMS, and CD spectra for new compounds and the figures of anti-tumor activity assay of CD8⁺ T cells in vitro.

File Name: Supporting Information

File Format: PDF

Title: Supporting Information of Non-peptide compounds from *Kromopolites svenhedini* (Verhoeff) and their anti-tumor and iNOS inhibitory activities

Acknowledgements

Funding

This study was supported financially by the Shenzhen Science and Technology Program (No. KQTD20210811090219022), the Shenzhen Fundamental Research Program (No. JCYJ20200109114225087, JCYJ20210324120213038), and the National Science Fund for Distinguished Young Scholars (No. 81525026).

References

1. Suzuki, Y.; Grayston, S.J.; Prescott, C.E. *Soil Biology & Biochemistry*, **2013**, 57, 116–123. DOI: 10.1016/j.soilbio.2012.07.020
2. Deng, M.D.; Gao, S.X. *Chinese Animal Medicine*, **1981**. ISBN: 14091-83
3. Stašiov, S.; Vician, V.; Benča, T.; Pätoprstý, V.; Lukáčik, I.; Svitok, S. *Acta Oecologica*, **2021**, 113, 103793. DOI: 10.1016/j.actao.2021.103793
4. Brown, S.P.; Brogden, M.; Cortes, C.; Tucker, A.E.; Snyder, B.A. *Soil Biology & Biochemistry*, **2021**, 159, 108285. DOI: 10.1016/j.soilbio.2021.108285
5. Bogyó, D.; Magura, T.; Simon, E.; Tóthmérés, P. *Landscape & Urban Planning*, **2015**, 133, 118–126. DOI: 10.1016/j.landurbplan.2014.09.014
6. Segura-Ramírez, P.J.; Godoy, P.J.; Avino, I. N.; Junior, P.I.S. *Journal of Proteomics*, **2021**, 242, 104239. DOI: 10.1016/j.jprot.2021.104239
7. Wood, F.W.; Hanke, F.J.; Kubo, I.; Carroll, J.A.; Crews, P. *Biochemical Systematics & Ecology*, **2000**, 28, 98–100. DOI: 10.1016/S0305-1978(99)00068-X
8. Weatherston, J.; Tyrrell, D.; Percy, J.E. *Chemistry & Physics of Lipids*, **1971**, 7, 98–100. DOI: 10.1016/0009-3084(71)90023-5
9. Bai, H.F.; Li, Y.P.; Qin, F.Y.; Yan, Y.M.; Cheng, Y.X. *Fitoterapia*, **2020**, 143, 104589.
10. Yan, Y.M.; Xiang, B.; Zhu, H.J.; Cheng, Y.X. *Journal of Asian Natural Products Research*, **2019**, 21, 93–102. DOI: 10.1016/j.fitote.2020.104589

11. Yan, Y.M.; Meng, X.H.; Bai, H.F.; Cheng, Y.X. *Organic Chemistry Frontiers*, **2018**, 21, 1401–1408. DOI: 10.1039/D0QO01653E
12. Li, J.; Li, Y.P.; Qin, F.Y.; Yan, Y.M.; Cheng, Y.X. *Fitoterapia*, **2020**, 142, 104534. DOI: 10.1016/j.fitote.2020.104534
13. Chen, H.; Yan, Y.M.; Wang, D.W.; Cheng, Y.X. *Molecules*, **2021**, 26, 3531. DOI: 10.3390/MOLECULES26123531
14. Ding, W.Y.; Yan, Y.M.; Meng, X.H.; Nafie, L.A.; Xu, T.; Dukor, R.K.; Qin, H.B.; Cheng, Y.X. *Organic Letters*, **2020**, 22, 5726–5730. DOI: [10.1021/acs.orglett.0c01593](https://doi.org/10.1021/acs.orglett.0c01593)
15. Padumadasa, C.; Xu, Y.M.; Wijeratne, E.M.K.; Espinosa-Artiles, P.; U'Ren, J.M.; Arnold, A.E.; Gunatilaka, A.A.L. *Journal of Natural Products*, **2018**, 81, 616–624. DOI: 10.1021/acs.jnatprod.7b00838
16. Liao, H.X.; Zheng, C.J.; Huang, G.L.; Mei, R.Q.; Wang, C.Y. *Journal of Natural Products*, **2019**, 82, 2211–2219. DOI: 10.1021/acs.jnatprod.9b00241
17. Jain, A.C.; Khanna, V.K.; Seshadri, T.R. *Tetrahedron*, **1969**, 25, 275–282. DOI: 10.1016/S0040-4020(01)82621-1
18. Ren, F.C.; Wang, L.X.; Yu, Q.; Jiang, X.J.; Wang, F. *Natural Products and Bioprospecting*, **2015**, 5, 263–270. DOI: 0.1007/s13659-015-0076-0
19. Cardona, M.L.; Fernández, I.; Pedro, J.R.; Serrano, A. *Phytochemistry*, **1990**, 29, 3003–3006. DOI: 10.1016/0031-9422(90)87123-C
20. Abdel-Lateff, A.; Klemke, C.; König, G.M.; Wright, A.D. *Journal of Natural Products*, **2003**, 66, 706–708. DOI: 10.1021/np020518b
21. Li, F.F.; Sun, Q.; Wang, D.; Liu, S.; Lin, B.; Liu, C.T.; Li, L.Z.; Huang, X.X.; Song, S.J. *Journal of Natural Products*, **2016**, 79, 2236–2242. DOI: 10.1021/acs.jnatprod.-6b00305
22. Augusta, M.M.; Ana, L.; Regina, T.M.; Marcelo, C.M.J.; Savluchinske, F.S.; José Carlos.Z. *Naturforsch*, **2006**, 61, 472–476. DOI: 10.1515/znc-2006-7-802

23. Kasai, R.; Fujino, H.; Kuzuki, T.; Wong, W.H.; Goto, C.; Yata, N.; Tanaka, O.; Yasuhara, F.; Yamaguchi, S. *Phytochemistry*, **1991**, 30, 2699–2702. DOI: 10.1016/0031-9422(86)80019-X
24. Trang, D.T.; Duong, D.T.; Nhiem, N.X.; Tai, B.H.; Yen, P.H.; Anh H.L.T.; Thung, D.C.; Minh, C.V.; Kiem, P.V. *Vietnam Journal of Chemistry*, **2016**, 54, 477. DOI: 10.15625/0866-7144.2016-00350
25. Tschritzis, F.; Jakupovic, J.; Bohlmann, F. *Phytochemistry*, **1990**, 29, 195–203. DOI: 10.1016/0031-9422(90)89036-9
26. Mori, K.; Murata, N. *Liebigs Annalen*, **1995**, 12, 2089–2092. DOI: 10.1002/jlac.-1995199512294
27. Luo, S.L.; Huang, X.J.; Wang, Y.; Jiang, R.W.; Wang, L.; Bai, L.L.; Peng, Q.L.; Song, C.L.; Zhang, D.M.; Ye, W.C.; *Fitoterapia*, **2014**, 95, 115–120. DOI: 10.1016/j.fitote.2014.03.004
28. Yang, Y.X.; Luo, Q.; Hou, B.; Yan, Y.M.; Wang, Y.H.; Tang, J.J.; Dong, X.P.; Ma, X.Y.; Yang, T.H.; Zuo, Z.L.; Cheng, Y.X.; *Journal of Asian Natural Products Research*, **2015**, 17, 988–995. DOI: 10.1080/10286020.2015.1047771
29. Yang, Y.X.; Meng, X.H.; Bai, H.F.; Cheng, Y.X.; *Organic Chemistry Frontiers*, **2021**, 8, 1401–1408. DOI: 10.1039/D0QO01653E
30. Yao, G.D.; Sun, Q.; Song, X.Y.; Huang, X.X.; Song, S.J. *Chemico-Biological Interactions*, **2018**, 289, 1–8. DOI: 10.1016/j.cbi.2018.04.014
31. Radivojevic, J.; Skaro, S.; Senerovic, J.; Vasiljevic, B.; Guzik, M.; Kenny, S.T.; Maslak, V.; Nikodinovic-Runic, J.; O'Connor, K.E. *Applied Microbiology & Biotechnology*, **2016**, 100, 161–172. DOI: 10.1007/s00253-015-6984-4
32. Frisch, M. J.; Trucks, G. W.; Schlegel, H. B.; Scuseria, G. E.; Robb, M. A.; Cheeseman, J. R.; Scalmani, G.; Barone, V.; Mennucci, B.; Petersson, G. A.; Nakatsuji, H.; Caricato, M.; Li, X.; Hratchian, H. P.; Izmaylov, A. F.; Bloino, J.; Zheng, G.;

Sonnenberg, J. L.; Hada, M.; Ehara, M.; Toyota, K.; Fukuda, R.; Hasegawa, J.; Ishida, M.; Nakajima, T.; Honda, Y.; Kitao, O.; Nakai, H.; Vreven, T.; Montgomery, J. A.; Peralta, J. E.; Ogliaro, F.; Bearpark, M.; Heyd, J. J.; Brothers, E.; Kudin, K. N.; Staroverov, V. N.; Keith, T.; Kobayashi, R.; Normand, J.; Raghavachari, K.; Rendell, A.; Burant, J. C.; Iyengar, S. S.; Tomasi, J.; Cossi, M.; Rega, N.; Millam, J. M.; Klene, M.; Knox, J. E.; Cross, J. B.; Bakken, V.; Adamo, C.; Jaramillo, J.; Gomperts, R.; Stratmann, R.E.; Yazyev, O.; Austin, A. J.; Cammi, R.; Pomelli, C.; Ochterski, J. W.; Martin, R. L.; Morokuma, K.; Zakrzewski, V. G.; Voth, G. A.; Salvador, P.; Dannenberg, J. J.; Dapprich, S.; Daniels, A. D.; Farkas, O.; Foresman, J. B.; Ortiz, J. V.; Cioslowski, J.; Fox, D. J. *Wallingford CT, 2010*.